Microsegregation and inclusion development during the casting of steel

A.A. Howe
Corus RD&T, Swinden Technology Centre, Moorgate, Rotherham S60 3AR &
Dept. of Engineering Materials, University of Sheffield, Sheffield S1 3JD, UK

Abstract

The enrichment of composition in the residual liquid during solidification is of itself an important parameter regarding the fitness for purpose of the alloy and, furthermore, will have a major influence on the precipitates and oxide inclusions that can nucleate and/or grow in the mushy zone. Corus sought a relatively simple, rapid model for this microsegregation and its associated inclusion type and size, for predictions across the thickness of continuously cast steels, suitable for use in conjunction with macro-models but demonstrably superior to the use of analytical equations. Notably, the analytical equations employ constant temperature equilibrium and diffusivity data for a process that can cover a very wide temperature range, and the assumed growth laws coupled with these data have an implied thermal history at odds with the environment of the macroscopic model within which the algorithm is to be used. The development and use of this model are described, along with its validation against a proven but time-consuming Finite Difference program for this purpose.

Keywords: Microsegregation, inclusion development, casting of steel.

1. Introduction

In certain steel grades, substantial changes in the oxide inclusions are noted between liquid steel and cast steel samples. The microsegregation process is the obvious explanation, and this was the particular focus of the work. However, this involved deriving a rapid routine for microsegregation calculation suitable for use in conjunction with macroscopic solidification models, and which could be used for other purposes as well.

Analytical equations of microsegregation are in common use, notably the equation of Clyne and Kurz [1], but these cannot handle temperature-dependent variables such as diffusivity, or address the effects of dendrite arm coarsening. Moreover, they can assume a growth rate and corresponding temperature-time history that is incompatible with that naturally resulting from the thermal environment. Numerical models can avoid these problems. Corus already has relevant numerical models, i.e. a Finite Difference model for microsegregation of multicomponent steels included the three-phase peritectic transformation [2,3], including dendrite arm coarsening according to an imposed law, and the MICRESS Phase Field model courtesy of a European Framework 5 project [4] for which the length-scale and geometry are part of the solution rather than required as input parameters. However, these are too time-consuming for use in conjunction with a macroscopic model. This paper describes Corus' model that avoids both the limitations of the analytical equations and the time requirements of the full, numerical models.

2. Basis of microsegregation model

Before describing how the limitations of analytical models can be avoided, it is useful to consider the derivation of the standard Clyne-Kurz formulation. In essence, it straddles the range of solute behaviour from the equilibrium lever-rule to the Scheil equation, according to a parameter dependent on the diffusivity. In differential form, the lever rule can be written as follows, where C_L is the concentration in the liquid, and the concentration in the solid at the interface is assumed to be given by kC_L where k is the partition coefficient, f is the fraction solid, and a raised "dot" signifies the time derivative:

$$C_l(1-k)\dot{f_s} = f_s k\dot{C_l} + (1-f_s)\dot{C_l} \qquad (1)$$

The Lever rule assumes a uniform increase of the solid composition to kC_l, as would be the case for an infinite diffusivity. A more realistic solute balance equation will include a "back diffusion" term of the solute flux away from the interface into the bulk solid according to a finite diffusivity. Treatment of finite diffusion requires treatment of an actual length-scale rather than a fraction solid, and the distance ordinate is represented here by r (the equations are easily modified for extension beyond 1D to a radius), with the diffusion coefficient given by D:

$$C_l(1-k)\dot{r} = D.\frac{dC}{dr} + (r_f - r)\dot{C_l} \qquad (2)$$

The Scheil equation, in differential form, results simply from setting D to zero. However, a more useful limit is that of Brody and Flemings [5], extendable to finite, low values of D, whereby the gradient in the concentration towards the interface (dC/dr) is considered equal to the gradient of the

concentration at the interface as the interface advances, i.e. kdC_L/dr. The resultant solute balance formula is therefore:

$$C_l(1-k)\dot{r} = D.k\frac{dC_l}{dr} + (r_f - r)\dot{C}_l \quad (3)$$

Clyne and Kurz [1] got around the restriction to low diffusivities by devising a back-diffusion term that varied from the equilibrium limit to the Brody-Flemings limit according to the diffusivity. Consider the differential form of the Lever rule, written in terms of distances, *r*, rather than fraction solid. Essentially, Clyne and Kurz added a factor, A, to the back-diffusion/solid enrichment term:

$$C_l(1-k)\dot{r} = Ark\dot{C}_l + (r_f - r)\dot{C}_l \quad (4)$$

This term, A, had to equal unity for infinite diffusivity and zero for zero diffusivity, but moreover, it had to tend to the Brody and Flemings solution at low but finite diffusivities. Noting that dC_l/dr in Equation 3 is equal to $\frac{dC_l}{dt}\cdot\frac{dt}{dr} = \frac{\dot{C}_l}{\dot{r}}$, then A must tend to $D/r\dot{r}$ at low values of *D* to render Equations 3 and 4 equal to each other. Clyne and Kurz assumed a parabolic growth law whereupon $r\dot{r}$ is constant, and which, combined with a constant diffusivity, allows the differential equation to be integrated analytically. They devised a rather complicated function to allow *A* to tend from zero to unity as *D* tends from zero to infinity. However, it was found [6] that a much simpler function corresponds to theirs very closely, and moreover, could be modified for other growth laws and geometries:

$$A = \frac{2\alpha}{1+2\alpha} \quad \text{where } 2\alpha = D/r\dot{r} \quad (5)$$

(In Clyne and Kurz' case with an assumed, parabolic growth rate, α was given by $\frac{1}{2}Dt_f/r_f^2$.)

This is the basis of the new model, but where *D* and $r\dot{r}$ are allowed to vary according to the variation in temperature, interactively compatible with the macroscopic actual or model environment. This merely requires the numerical, macroscopic model to perform sufficient iterations for this microsegregation routine to produce a stable answer, rather than an answer that still varies according to the number of iterations. The interaction is through the heat balance equation.

$$\dot{Q} = H\dot{f}_s + C_P.\dot{T} \quad (6)$$

where dQ/dt is the heat extraction rate, *H* is the latent heat, C_P is the specific heat capacity (whether approximated as being equal for the solid and liquid or weighted according to their volume fractions if different values of C_P per phase are employed, and df_s/dt is given by $(dr/dt)/r_f$. Assuming liquidus depressions are additive, as has been shown to be very successful up to medium alloy steels [7] and where m_i is the liquidus slope, dT/dC_l, for the solute *i*:

$$T = T_o - \sum_i m_i C_{l,i} \quad (7)$$

Then the suite of equations is readily solved for an arbitrary number of solutes without recourse to time-consuming iteration with thermodynamic software. In addition, the effect of arm coarsening can be included according to a known, imposed law. The core solute balance is extended as follows [8]:

$$C_l(1-k)\dot{r} = D.\frac{dC}{dr} + (r_t - r)\dot{C}_l + (C_l - C_0)\dot{r}_t \quad (8)$$

where r_t is the size of the representative cell at time, t. The r_f term employed previously has to be changed to this new parameter, as it is no longer the final value. With r_t imposed according to an equation only of time, *t*, this does not introduce any further unknown parameters. Typically this would take the form $r_t = Gt^{1/3}$ where G is an empirical constant.

Summing terms for the various solutes that might be present and substituting into Equation 6, yields the following equation to be solved at each iteration of the macroscopic model:

$$\dot{Q} = \left\{\frac{H}{r_t} - C_P\sum_i \frac{m_i C_{l,i}(1-k_i)}{(r_t - (1-A_i k_i)r)}\right\}.\dot{r} - \left\{\frac{H.r}{r_t^2} - C_P\sum_i \frac{m_i(C_{l,i} - C_{0,i})}{(r_t - (1-A_i k_i)r)}\right\}.\dot{r}_t \quad (9)$$

With the growth rate determined according to a known heat extraction rate, the terms dC_{li}/dt and thence dT/dt can all be determined from the above equations, and *r*, $C_{l,i}$ and *T* can be updated in first-order fashion according to the time increment employed for the calculations.

3. Growth of inclusions

The model addresses the worst case that should be expected from inclusion development in the mushy zone, i.e. with a suitable seed present to avoid any nucleation problems, and the size and composition of the inclusion being that expected from equilibration of the residual liquid. The procedure is thus straightforward. At each iteration, the residual liquid composition is compared with solubility product formulae for the relevant range of oxide species involving one or more of silicon, manganese and aluminium. If a particular oxide is identified as being stable, its size is calculated from the amount of its component elements present in the residual liquid. Within a well-formed columnar zone, the residual pool size is taken to be that of a volume corresponding to the secondary dendrite arm spacing. Within the more chaotic structure of the equiaxed zone, it is arguable that a larger volume should be considered because of the more ready percolation between dendritic interstices. That would be a time-consuming modelling exercise in itself, and for present purposes a 50% increase in diameter is assumed, corresponding to the sourcing of material from a little over three dendritic interstices.

4. Validation

The in-house Finite Difference model had already been successfully validated against experiment [3] and microsegregation models derived at other institutes [3,9]. This, therefore, formed the basis for testing of the streamlined model.

A time-dependent law for the secondary dendrite arm coarsening behaviour has to be known, for the current example being a simple cube-root time law consistent with standard expectation [8] and fitted to experimental data for the grades and casting machines in question. The same law is then used in the calculation throughout the cast section, with the amount of coarsening and inclusion growth therefore limited by the local solidification time as calculated by the macro/micro model.

An initial test for any iterative model is that the result converges on a consistent answer with successive refinement of the iterative step size (time-step). Moreover, to be of use, it should do so at a sufficiently coarse step size to keep the number of iterations reasonable and the run-time thereby very short. Of course, the converged solution should also

be a close approximation to that obtained from the original FD model. The streamlined model typically reached a predicted, depressed solidus temperature within a fraction of a degree of the "infinite iterations" result within a fraction of a second's run time. In Figure 1, an example is given of the convergence of the calculated results with decreasing step size.

It can be seen that the streamlined model converges for time-steps below about 10 s in this case of a ~ 660 s local solidification time, onto values within 2.5% of the full, Finite Difference solution. In Figure 2, example calculations are presented of the match between the streamlined model and the full FD model with increasing fraction solid. It can be seen that the development of carbon content is almost identical: the value of A in the streamlined model is high enough for the calculations to follow closely the equilibrium result, and the FD model assumes equilibrium for this element [3]. The streamlined model slightly overestimates the enrichment of silicon and underestimates the enrichment of manganese, but both within a few percent of the FD result until the very end of solidification, at the very sensitive calculation of the depressed solidus where the silicon enrichment is overestimated by about 10%. In absolute terms these differences are still rather small and, moreover, for the current concern of inclusion development in the mushy zone, the last few percent of solidification are not very important. Accordingly, the selection of inclusion species and the potential size that the inclusions could reach are essentially identical between the two models.

Actual sizes and frequency of occurrence of the potential, maximum sizes of inclusions are commercially sensitive data, but an illustration is presented here of the relative sizes calculated for two different caster configurations to demonstrate the application of the streamlined model in this regard, in Figure 3.

5. Discussion

The streamlined model has been shown to offer surprisingly good agreement with the full, FD model, and is thereby suitable for use in conjunction with macro-models. It predicts data on microsegregation and inclusion type/size information forming in the mushy zone, across the width and/or thickness of the cast section, which would invoke a prohibitive time requirement using the FD model.

However, various limitations should be noted:

i. Nucleation is not addressed. Homogeneous nucleation is very unlikely, so some, albeit tiny, "seed" oxide is probably required. This will result in otherwise equivalent interdendritic interstices exhibiting anything

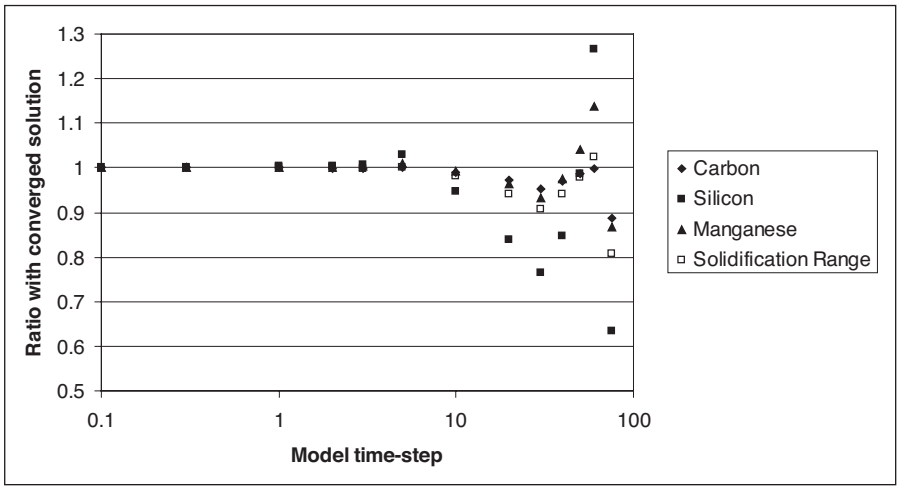

Figure 1: Model convergence as a function of time-step (local solidification time ~660 s).

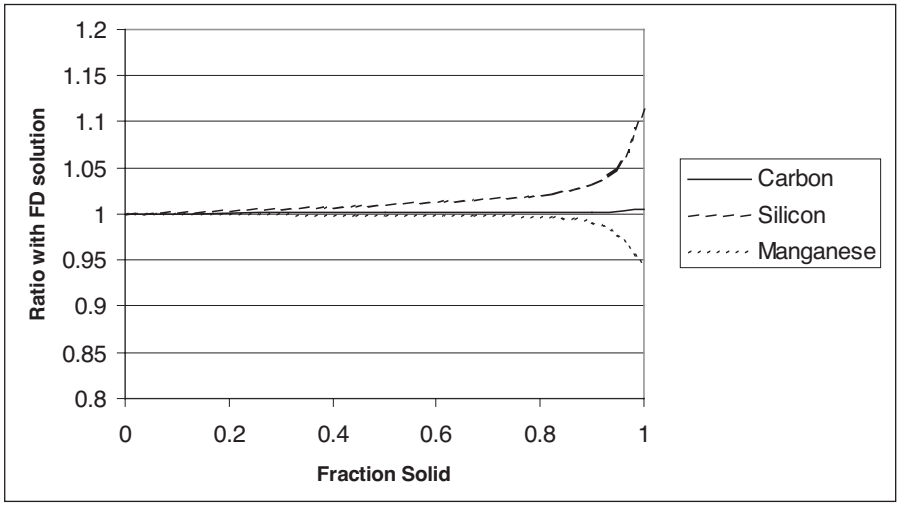

Figure 2: Example of the model divergence from the predictions of the full FD calculations versus fraction solid.

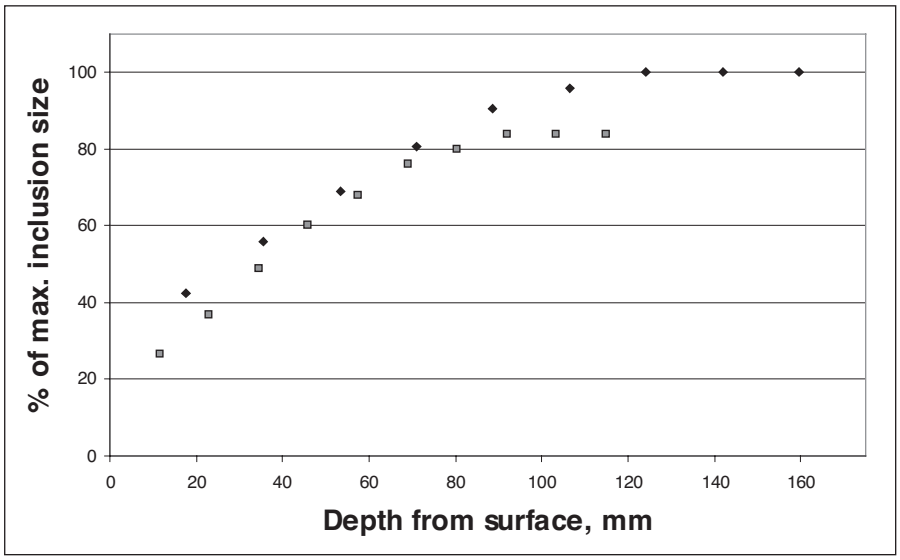

Figure 3: Relative potential inclusion sizes calculated for alternative caster configurations.

from no oxide particle up to the maximum particle size predicted by the model.

ii. No automatic differentiation is made between the columnar and equiaxed zones. For the former, the region from which material can be sourced for the growth of an individual oxide is likely to be one interdendritic pool, whereas in the more chaotic equiaxed zone, this feeding ground is likely to be larger. Currently, this effect is taken to approximately counter the reduced size at the centre that is otherwise expected of the observed "double-hump" profile of dendrite arm spacings across the casting.

iii. Macrosegregation spots or channels are not addressed: potentially these could promote larger inclusions and/or different chemistries.

iv. Substantial, pre-existing inclusions are not addressed, i.e. any that might be present prior to solidification.

v. Currently, a single solidification phase is addressed, although work is in hand to extend the model to three phases and the peritectic transformation.

Regarding the last two, attention should be paid to their avoidance rather than to modelling their effects, but the micro model can be readily adapted to predict the result for a known macrosegregate or assimilation with a known exogenous inclusion. Regarding the first two, the predictions are considered to be satisfactory and useful for the case described here.

6. Conclusions

A streamlined microsegregation model is presented, suitable for use within a macroscopic model of solidification, which allows for multiple solutes with widely differing diffusivities, temperature-dependent thermodynamic/diffusive data, and secondary dendrite arm coarsening, whilst avoiding imposed thermal histories that can be inconsistent with the natural thermal history for the combined micro/macro model. Excellent agreement is observed with a time-consuming, Finite Difference model. Its particular use highlighted here is for the prediction of the type and maximum size of inclusion expected to develop within the mushy zone during solidification, for which it is proving very useful.

References

1. Clyne, T.W. and Kurz, W., Met. Trans. A, 1981, **12A**, 965.
2. Howe, A.A., in: Procs. Internat. Confs. on Solidification Processing, Sheffield, 1987, pp. 63–65 and 1997, pp. 312–315, publ. University of Sheffield.
3. Howe, A.A. and Kirkwood, D.H.: "Computer prediction of microsegregation in peritectic alloy systems", Mater. Sci. Technol., 2000, **16**, 961–967.
4. Howe, A.A. *et al.*: "Virtual experiments to solve problems in steel metallurgy", final summary report, Framework 5 Contract GRD1-2000-25447.
5. Brody, H.D. and Flemings, M.C., Trans. Met. Soc. AIME, 1966, **236**, 615.
6. Howe, A.A.: "Extension of analytical expressions for microsegregation", Ironmaking and Steelmaking, 1991, **18** No.4, p. 284.
7. Miettinen, J. and Howe, A.A.: "Estimation of liquidus temperatures for steels using thermodynamic approach", ibid, 2000, **27** No.3, p. 212.
8. Kirkwood, D.H., Mater. Sci. Eng., 1984, **65**, 101.
9. Schulze, Th., Wendt, J. and Howe, A.A., in: 'COST 512 Workshop, Modelling in Materials Science and Processing', Publ. European Commission, 1996. ■